Contents lists available at SciVerse ScienceDirect

CIRP Annals Manufacturing Technology

Journal homepage: www.elsevier.com/locate/cirp

Position sensor for active magnetic bearing with commercial linear optical encoders

Mathias Tantau[ad], Paul Morantz[abc], Paul Shore[abc]

[a] *Precision Engineering Institute, SATM, Cranfield University, United Kingdom*
[b] *Loxham Precision Ltd., United Kingdom*
[c] *National Physical Laboratory, United Kingdom*
[d] *Leibniz University Hannover, Germany*

Submitted by Prof. David Allen, Cranfield University

Active magnetic bearings are used in a number of applications but their disadvantage is the high asynchronous error due to sensor noise amplification. In this paper a new radial position sensor for active magnetic bearings (AMB) based on linear optical encoders is presented. A commercial encoder scanning head faces a round scale with concentric, coplanar lines on its face. Because such a scale is not readily available, it is made by high precision micro machining and different options are compared. In experiments a measurement noise of 3.5 nm at 10 kHz bandwidth is achieved. In addition, a magnetic bearing is built to demonstrate the sensor in closed-loop.

Magnetic Bearing, Encoder, Micro machining.

1. Introduction

Active magnetic bearings (AMBs) have the advantage over passive bearings that they can actively compensate imperfections of the mechanical structure which makes them interesting for machine tools, printing machines, high speed spindles, etc. In [1] AMBs correct straightness errors of a machine guideway and the rotary magnetic bearing in [2] eliminates undesired movements due to tool axis misalignment errors. In CNC machines active damping prevents chatter [3]. Magnetic bearings in printing machines could serve the film steering [4], provide an adjustable force profile [5] or they could be used for process monitoring [6].

Unfortunately, the applicability of radial AMBs to high precision applications is limited by the unavoidable asynchronous error and the low stiffness at medium frequencies [3]. A prerequisite for a high bearing stiffness is a position sensor with low noise and at the same time high bandwidth [7]. Sampling rates of about 10 kHz are necessary in magnetic bearings because control bandwidth and stiffness are restricted by time delays [8]. The asynchronous error of an AMB is equally determined by the sensor noise [7, 9]. For these two reasons AMB position sensors must feature as low noise as possible.

There are largely four types of sensors to measure the lateral shaft position in radial AMBs: capacitive, eddy current, inductive and electro-optical [9]. The range to resolution ratio of these sensors is particularly important. Representative is the radial bearing in [2] with 2×300 µm air gap. For such a bearing a position sensor with at least 600 µm range would be required, better 1000 µm. A high quality capacitive sensor from Lion Precision [10] or Micro-Epsilon [11] with this range would have approximately 20 nm RMS resolution at 10 or 15 kHz bandwidth.

Capacitive sensors in AMBs are disturbed by electromagnetic interference (EMI) and the rotor should be grounded [11]. The other sensor types are less susceptible to EMI, but their nominal resolution is inferior and they have other limitations: Eddy current sensors are affected by target material inhomogeneity, inductive sensors have hysteresis and electro-optical sensors with CCDs have limitations due to diffraction [7, 10]. Most gap sensors are not optimized for measurements on a curved shaft and surface imperfections lead to additional errors [12].

In this paper a novel position sensor for radial magnetic bearings based on linear optical encoders and a circular scale disc is performed that combines high resolution and EMI immunity. The encoder scale is made by micro-machining. Experimental results with different cutting procedures are compared, the sensor is tested on its own and finally in closed-loop position control in a magnetic bearing.

2. Radial position measurement with linear optical encoders

2.1. Principle of operation with amplitude gratings

A schematic of the envisioned magnetic bearing spindle is shown in Figure 1. Two incremental linear optical encoder scanning heads count concentric, coplanar lines on the face of each scale disc on the shaft. This allows to measure the lateral position of the shaft as a feedback for the radial AMB control. The discs are mounted in two distinct positions along the shaft, corresponding to the two radial magnetic bearings. A similar approach, albeit with radial gratings and rotary encoders is described in [13]. The circular grating approach may be superior at high speed of rotation and it works without subtracting two measurements so that the noise amplification effect could be avoided.

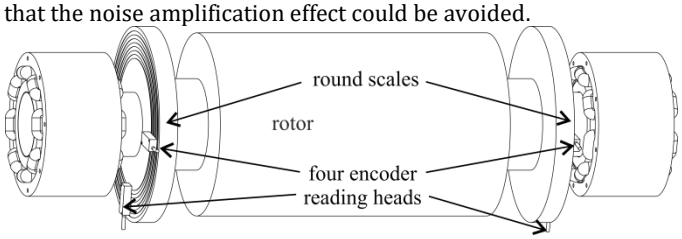

Figure 1. Schematic of lateral position measurement in radial AMB

The encoder scanning heads can be bought as they are ordinary linear encoders, but the displayed round scales are not commercially available and a procedure must be found for machining them with high precision and suitable grating contrast. Usually the gratings on encoder scales are made by means of photolithography, etching and vapour deposition [14], but making the new scale with these techniques would require

'extremely specialized and costly equipment and procedures' [15], p. 334 and the correct process parameters are hard to find. Most importantly it would be difficult to align the lithography masks concentric with the rotor axis; a lateral offset is expectable, causing armature run-out errors. Our approach is to cut the gratings with a high precision diamond turning lathe into a strong metal disc. The exact procedure needs to be established.

The two exposed linear encoder scanning heads AK LIDA 28 and AK LIDA 48 from Heidenhain are chosen as potential candidates for the reading heads. As they are both based on the 'imaging scanning principle', they require a scale with amplitude gratings, no phase gratings [14] and more specifically alternating reflective and absorbent lines with 1:1 division ratio. For type LIDA 28 the pitch or grating period is 200 µm and for LIDA 48 it is 20 µm, dictated by the reading head. Together with the reticle in the scanning head a moving wave is created, the phase of which is evaluated over a continuous area of 14.5 mm^2 under the reading head. This phase embodies the incremental position and is communicated in two 90° phase shifted sine signals. The peak-to-peak amplitude of these signals indicates the imaging quality, ideally 1 V_{PP} [14].

2.2. Derivation of implications associated with curved scale

Since the reading heads are optimized for scales with straight lines, the signal quality, measured by amplitude A, will degrade when our curved lines are evaluated. This effect will be amplified when the spindle moves out of centre due to motions in the second radial axis. Figure 2 illustrates the encoder reticle hovering over the scale, which is offset from the centre by x_c. Because of the scale curvature each grey scale line, index n is phase shifted with respect to the corresponding reticle line for position x:

$$\varphi_n(x) = \frac{2\pi}{p}\left\{R_i + np - \sqrt{(R_i + np)^2 - x^2}\right\}. \qquad 2.1$$

The accumulative peak-to-peak amplitude A of all m grooves together follows from integration over the reading head width l_x:

$$A = \frac{1}{ml_x}\left|\sum_{n=0}^{m-1}\int_{x_c-\frac{l_x}{2}}^{x_c+\frac{l_x}{2}} e^{j\cdot\varphi_n(x)}\mathrm{d}x\right|\cdot A_{max}. \qquad 2.2$$

Quantity A_{max} is the peak-to-peak amplitude with ideal, parallel lines.

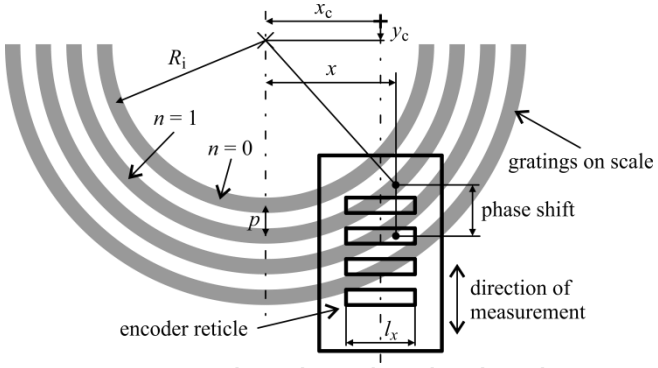

Figure 2. Linear encoder tracks circular scale with misalignment

In addition to the deterioration of signal quality the misalignment error causes a certain, well defined measurement error related to the curved scale. When the scale is not centred horizontally, a false measurement of approximately $\frac{p}{2\pi}\varphi_{m/2}(x_c)$ occurs. This effect is comparable to ordinary gap sensors, where a round shaft is the sensor target. Here, the effect is less pronounced because the scale can be of large diameter.

3. Experimental procedures

3.1. Micro machining of scale discs and open-loop sensor experiments

The concentric grooves are cut with a Nanotech 350UPL diamond turning lathe from Moore Technology Systems into aluminium discs, grade 6061-T6 with 120 mm diameter and 29 mm thickness. Diamond turning of aluminium with this machine creates even surfaces with mirror finish and $R_a \approx 5$ nm, which become the reflective lines of the amplitude gratings. The grating rings can be produced highly concentric with other surfaces of the disc, facilitating the alignment in the AMB.

Three procedures for structuring the surface are sketched in Figure 3. For profile (a) the surface is levelled out first and then a pointed tool cuts V-grooves, in which the incident light is supposed to be trapped.

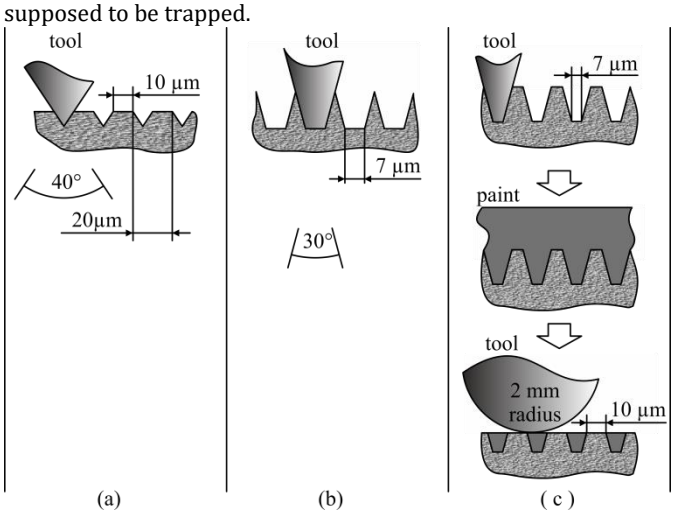

Figure 3. Three procedures for micro-machining of amplitude gratings

Because the burr formation at the margins of the grooves might impose a problem, profile (b) is made with a flat tool and the light is expected to be reflected at the bottom of the grooves and burr might be less decisive. Profile (c) utilizes a flat tool for the structuring, then blackboard paint is applied and finally a round diamond tool clips aluminium and paint leaving a division ratio of ideally 1:1 between the reflective aluminium and the rough and absorbent paint.

In Figure 3 only the 20 µm grating period versions of the three profiles are shown; the 200 µm counterparts for the other encoder work equivalently, albeit with different dimensions.

For testing each machined scale with encoder reading head the scale is clamped on the vacuum chuck of the same machine again and the reading head is attached to the tool holder of the machine as displayed in Figure 2 with either displacement x_c or displacement y_c adjustable by the machine's spindle positioning system.

The encoder output signals are recorded with rapid prototyping equipment from the company Speedgoat and the ADC board IO106 at 10 kHz. An operational amplifier circuit in front of the ADC converts the differential encoder signals U^+ and U^- into a single-ended voltage, amplifies low frequencies by a factor of 3.92 and attenuates noise above 18.5 kHz. Its output is:

$$Y(j\omega) = \frac{3.92}{j\omega\cdot 8.62\ \mu s+1}\left(U^+(j\omega) - U^-(j\omega)\right). \qquad 3.1$$

3.2. Magnetic bearing demonstrator with encoders and gap sensors

In addition, a radial magnetic bearing has been built to demonstrate the position sensor in closed loop, see Figure 4. It is placed inside a Nanocentre diamond turning machine from the company Cranfield Precision. The left end of the shaft is

connected to the machine spindle via flexible coupling for 4DOF constraint including rotary motion control. On the right two linear encoder scanning heads face a ⌀300 mm scale disc with profile (a), 20 µm grating period applied to an electroless nickel coating on aluminium substrate. In this way nickel is machined, not aluminium, giving better machining properties. Between encoder reading heads and shaft, capacitive and eddy current gap sensors are mounted as an alternative measurement device to compare the performance.

For the control hardware a Performance real-time Target Machine from Speedgoat including IO106 ADC board and IO111 DAC board samples at an update rate of 10 kHz. The encoders are connected as explained above and the power drives are BA30 switching amplifiers from the company Aerotech.

The control can be described as decentralized PID with constant current sum and compensation of negative bearing stiffness. This simple and proven approach should be sufficient at low speed [7].

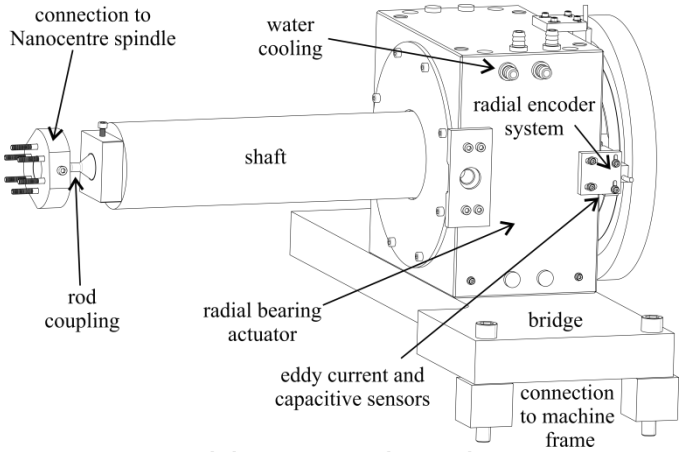

Figure 4. Radial 2DOF magnetic bearing demonstrator

4. Results

First, the results of microscope investigations and open-loop experiments on the Nanotech 350UPL are shown, followed by magnetic bearing experiments.

4.1. Encoder scale grating manufacture

Figure 5 shows four microscope pictures of machined gratings with 20 µm and 200 µm grating period. The profile identifiers refer to Figure 3. Clearly profiles (a) and (b) did not form properly because in the case of (a) burr has piled on the margins of the grooves, covering most of the reflective, flat surfaces between the grooves. As for profile (b) the cutting tool has shifted excess material into adjacent grooves and only the last groove, shown at the bottom of the subfigure, looks as intended. Both versions of profile (c) look promising and homogeneous over the entire raster area. There are only minor scratches in the aluminium and the aspect ratio of dark and bright is close to 1:1, deviations resulting from the cutting depth tolerances.

Table 1 gives an overview of the resolutions achieved with the four grating discs from Figure 5 in experiments at zero rotational velocity and the experimental setup described in section 3.1. This result reflects the expectations from the microscope pictures and in general the 20 µm gratings outperform the 200 µm ones in this respect.

As a next step, the encoder disc is moved slowly along y by the Nanotech 350UPL positioning system and the Lissajous figure from the encoder outputs is recorded, see Figure 6, left. Only the results for the two versions of profile (c) are shown, because this technology has turned out to produce the best results in the above experiment. The Lissajous is almost perfectly round.

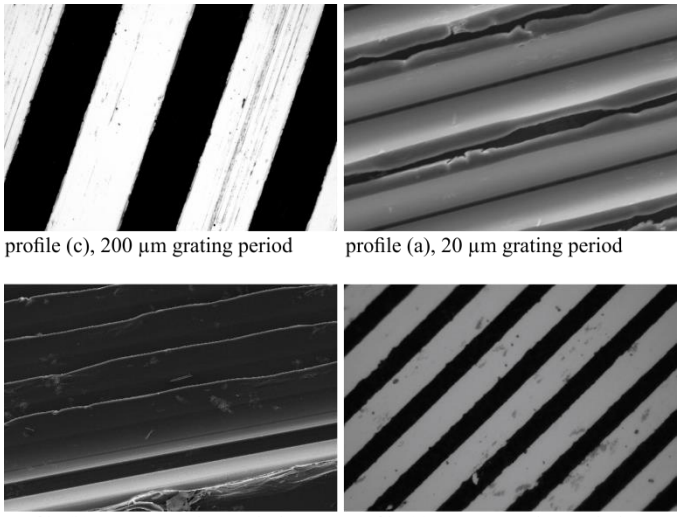

Figure 5. Microscope images of the four machined amplitude gratings

Table 1: Sensor noise in static experiment with encoders, root mean square (RMS) and peak-to-peak (p-p)

profile	c, 200 µm	a, 20 µm	b, 20 µm	c, 20 µm
RMS noise	13.8 nm	6.37 nm	19.6 nm	3.37 nm
p-p noise	139 nm	58.9 nm	189 nm	148 nm

What is not included in the noise measurements of Table 1 is the situation when the round scale is rotating. This is particularly interesting for rotary magnetic bearings that levitate rotors, but is not easy to quantify. The right graphic of Figure 6 is a position measurement with optical encoders while the scale is rotating at 60 rpm. A remaining runout from clamping the disc on the machine's vacuum chuck of approximately 2 µm causes an undulation at the rotational frequency. Tolerances in this range are expectable from manual alignment with an analogue dial indicator but it is a coincidence that both discs where clamped with the same runout. So, this 1 Hz undulation is not related to the measurement device. Deviations from the sinusoidal form can be attributed to scale roundness errors, especially for 200 µm (black) they form a highly repeatable pattern.

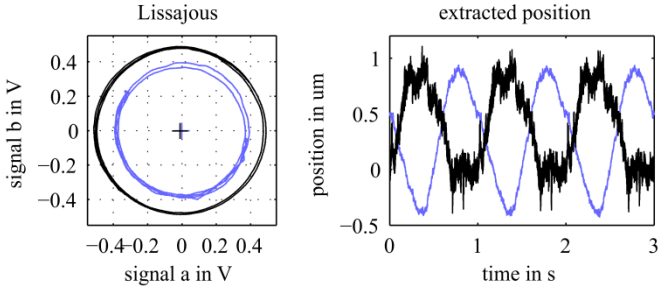

Figure 6. Lissajous and position tracking with 20 µm (blue) and 200 µm (black) gratings

As explained in section 2.2, the Lissajous diameter decreases when the rotor departs from the exact geometric centre. Figure 7 allows a comparison of the predictions according to (2.2) and the measurements. They are in good agreement, albeit with an offset in the 20 µm case. This offset might be related to the reduced reflectivity of the fine grating that was not taken into consideration in the calculation. It can be seen that the fine grating is more sensitive to misalignment errors and that this is a

range limitation comparable to that of capacitive sensors or eddy-current sensors.

4.2. Magnetic bearing results

Control of magnetic bearings with the proposed amplitude grating technique works as intuitive and reliable as with conventional gap sensors. In Figure 8 the positioning noise of the non-rotating radial active magnetic bearing is shown in the frequency domain. The noise has been recorded while the AMB was controlled with eddy current sensors, capacitive sensors or encoders respectively for radial position measurement.

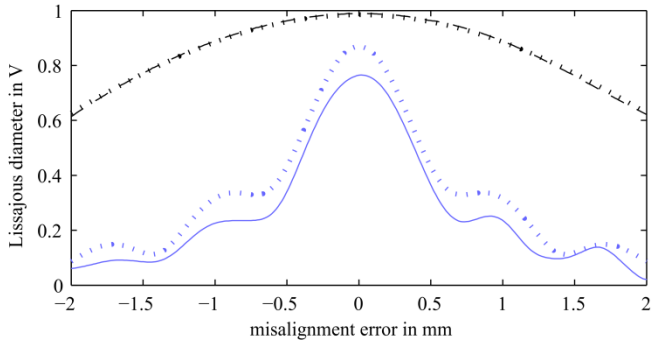

Figure 7: Signal strength reduction due to misalignment for profile (c) in 20 µm (blue) and 200 µm (black), measured (cont.) and calculated (dash)

At frequencies above 6 kHz the noise floor is much lower with encoders than with conventional sensors, which shows the noise reduction thanks to the proposed measurement device. At lower frequencies all three techniques show a similar noise in active control. Further investigations have shown that the peak at 50 Hz is related to the power amplifiers and that the resonance - anti-resonance around 2 kHz is related to flexible modes in the support structure. Naturally, these properties are not affected by the position sensors.

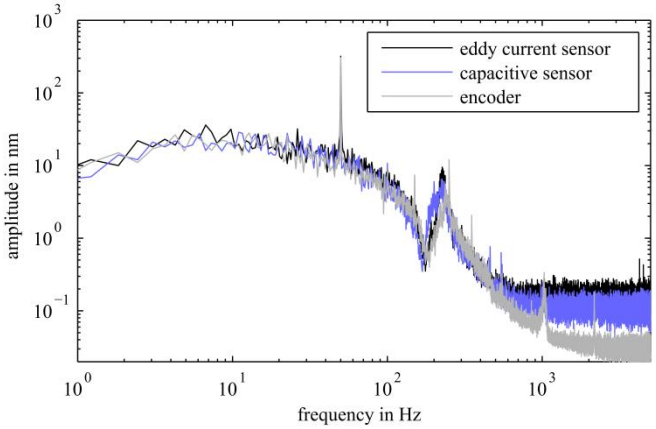

Figure 8: Positioning noise of the active magnetic bearing control with encoders in contrast to conventional gap sensors

In Table 2 the uncertainty levels achieved with different sensors are compared. To give a more complete overview the damping is also varied. These numbers that are determined from all frequencies together do not show a clear dependence on the sensor technology.

Table 2: ABM positioning noise for different sensors in µm

damping	eddy current		capacitive		encoder	
D	RMS	p-p	RMS	p-p	RMS	p-p
0.3	1.02	5.03	0.89	4.52	0.89	4.49
0.5	0.55	3.10	0.51	3.13	0.51	2.82
0.7	0.40	2.74	0.41	2.57	0.37	2.19

5. Conclusions / discussions

An innovative position sensor for radial magnetic bearings has been described and verified in experiments on a magnetic bearing to test the performance in open and closed loop. The advantage of this incremental principle is its very low noise in relation to the undiminished range of movement and high bandwidth. In closed-loop magnetic bearing control the performance was comparable to that of more expensive gap sensors. Unfortunately the dynamic control accuracy was not outstanding because of other factors such as amplifier noise and imperfections in the mechanical design.

The findings should be seen as a first prove of principle. Further design optimisation is planned to clarify for example the exact effect of EMI and temperature changes. High interpolation of analogue signals is delicate but is a standard practice using the type of encoders proposed. Optimisation of grating design is an established industry capability.

Also, the manufacturing of encoder discs should be further optimized in terms of tool geometry and materials and further validation experiments could be carried out.

This research is particularly interesting for facilities where diamond turning machines are available. The required materials are easy to buy and cheap, but the manufacture would be expensive if it could not be made in house.

Acknowledgements

EPSRC Centre for Innovative Manufacturing in Ultra Precision (EP/I033491/1)

Integrated Knowledge Centre in Ultra Precision and Structured Surfaces (EP/E023711/1)

References

[1] Kim O-S, Lee S-H, Han D-C. Positioning Performance and Straightness Error Compensation of the Magnetic Levitation Stage Supported by the Linear Magnetic Bearing. IEEE Transactions on Industrial Electronics. 2003; 50(2): pp. 374–378.

[2] Lee C-W, Yoon Y-K, Jeong H-S. Compensation of Tool Axis Misalignment in Active Magnetic Bearing Spindle System. KSME International Journal. 1997; 11(2): pp. 155–163.

[3] Denkena B, Guemmer O, Floeter F. Evaluation of electromagnetic guides in machine tools. CIRP Annals - Manufacturing Technology. Elsevier, Amsterdam, Netherlands; 2014; 63(1): pp. 357–360.

[4] Müller S, Schaudt H, Trajkovic D. DE 102005016779 A1: Flat multilayer commodity punching device for use in printing machine, has punching and counter punching cylinders, in which one is held in radially shiftable magnetic bearing to adjust breadth of punching gap between cylinders. DE patent; 2005.

[5] Bechtler J, Spilger R. DE10152839 A1: Positioning method for printing machine roller using control or regulation of roller magnetic bearing devices. DE patent; 2002.

[6] Förch P, Henn A. US 6604739 B2: Method and device for aligning flat copies in sheet-processing machines. US patent; 2003.

[7] Bleuler H, Cole MOT, Keogh PS, Larsonneur R, Maslen EH, Nordmann R, et al. Magnetic Bearings. Schweitzer G, Maslen EH (eds.) Springer, Berlin Heidelberg, Germany; 2009.

[8] Jabben L. Mechatronic Design of a Magnetically Suspended Rotating Platform. Delft, Netherlands: Technical University Delft; 2007.

[9] Sridharan G. Electro-Optical Position Measurement for Active Magnetic Bearing. Review of Scientific Instruments. 1985; 56(1): pp. 142–145.

[10] Lion Precision. Noncontact Displacement Sensors. 2015. Available at: http://www.lionprecision.com/

[11] Micro-Epsilon. Sensors & Measurement Systems. 2015. Available at: http://www.micro-epsilon.co.uk/index.html

[12] Fleming AJ. A review of Nanometer Resolution Position Sensors: Operation and Performance. Sensors and Actuators A: Physical. 2013; 190: pp. 106–126.

[13] Lu X, Dyck M, Altintas Y. Magnetically levitated six degree of freedom rotary table. CIRP Annals - Manufacturing Technology. 2015; 1(64): pp. 353–356.

[14] Dr. Johannes Heidenhain GmbH. Exposed Linear Encoders. 2014. Available at: https://www.heidenhain.de/fileadmin/pdb/media/img/1172234-20_Exposed_linear_encoders.pdf

[15] Davies MA, Dutterer BS, Suleski TJ, Silny JF, Kim ED. Diamond Machining of Diffraction Gratings for Imaging Spectrometers. Precision Engineering. 2012; 36(2): pp. 334–338.